

Systematic Study of L -Shell Opacity at Stellar Interior Temperatures

T. Nagayama,¹ J. E. Bailey,¹ G. P. Loisel,¹ G. S. Dunham,¹ G. A. Rochau,¹ C. Blancard,² J. Colgan,³ Ph. Cossé,² G. Faussurier,² C. J. Fontes,³ F. Gilleron,² S. B. Hansen,¹ C. A. Iglesias,⁴ I. E. Golovkin,⁵ D. P. Kilcrease,³ J. J. MacFarlane,⁵ R. C. Mancini,⁶ R. M. More,^{1,*} C. Orban,⁷ J.-C. Pain,² M. E. Sherrill,³ and B. G. Wilson⁴

¹Sandia National Laboratories, Albuquerque, New Mexico 87185, USA

²CEA, DAM, DIF, F-91297 Arpajon, France

³Los Alamos National Laboratory, Los Alamos, New Mexico 87545, USA

⁴Lawrence Livermore National Laboratory, Livermore, California 94550, USA

⁵Prism Computational Sciences, Madison, Wisconsin 53711, USA

⁶University of Nevada, Reno, Nevada 89557, USA

⁷Ohio State University, Columbus, Ohio 43210, USA



(Received 7 March 2019; published 10 June 2019)

The first systematic study of opacity dependence on atomic number at stellar interior temperatures is used to evaluate discrepancies between measured and modeled iron opacity [J. E. Bailey *et al.*, *Nature (London)* **517**, 56 (2015)]. High-temperature (> 180 eV) chromium and nickel opacities are measured with $\pm 6\%$ – 10% uncertainty, using the same methods employed in the previous iron experiments. The 10% – 20% experiment reproducibility demonstrates experiment reliability. The overall model-data disagreements are smaller than for iron. However, the systematic study reveals shortcomings in models for density effects, excited states, and open L -shell configurations. The 30% – 45% underestimate in the modeled quasicontinuum opacity at short wavelengths was observed only from iron and only at temperature above 180 eV. Thus, either opacity theories are missing physics that has nonmonotonic dependence on the number of bound electrons or there is an experimental flaw unique to the iron measurement at temperatures above 180 eV.

DOI: [10.1103/PhysRevLett.122.235001](https://doi.org/10.1103/PhysRevLett.122.235001)

Opacities quantify photon absorption in matter and are important for high-energy-density (HED) plasma simulations. HED plasma opacity is challenging to calculate and to experimentally validate. Because of a lack of benchmark experiments, opacity-calculation accuracy has sometimes been suspected as a source of disagreement between astronomy observations and models. For example, in 1982 Simon requested [1] reexamination of opacity calculations for Cepheid variable stars. In response, new models were developed [2–6] that raised calculated opacities by ~ 3 times for stellar envelopes and resolved the Cepheid variable problems. This precedent, combined with insufficient laboratory experiments to fully test the theory, has led to continued speculation that models may underestimate opacity for variable stars [7–9].

Recently, an inaccuracy of calculated solar interior opacity was proposed as a potential explanation for disagreement between solar models and helioseismology [10,11]. The opacity at the electron temperature $T_e \sim 182$ eV (2.11×10^6 K) and density $n_e \sim 9 \times 10^{22}$ cm $^{-3}$ that exist near the solar convective and radiative zone boundary (CZB) is especially important. To test this hypothesis, frequency-resolved iron opacity was measured at $T_e = 155$ – 195 eV and $n_e = (7$ – $40) \times 10^{21}$ cm $^{-3}$ [12,13] (hereafter BNL15). The modeled and measured

Fe opacities agreed reasonably well at the lowest T_e and n_e , but models underpredict the opacity in several ways as T_e and n_e approach CZB conditions. First, the calculated quasicontinuum opacity below 9 Å is 30% – 45% lower than measured. Second, calculated bound-bound (BB) transitions appear stronger and narrower than the measurements. Third, opacity valleys (windows) are lower in the calculations. All three discrepancies contribute to lower calculated Rosseland-mean opacity. If the measurements are correct, this explains roughly half the opacity increase needed to resolve the solar problem. However, solving the solar problem ultimately relies on benchmarked opacity models. The required opacities for a wide range of elements and conditions cannot be provided by measurements alone. The goal of the work described here is testing hypotheses for the model-data discrepancy.

Hypotheses for the source(s) of the discrepancies fall into two categories: (i) there are undetected flaws in the experimental method and/or (ii) photon absorption in HED matter is more complex than previously believed. Neither possibility can be ruled out until experiment and theory are reconciled. Experimental [11,14–18] and theoretical investigations [19–24] done up to now have not resolved the discrepancy.

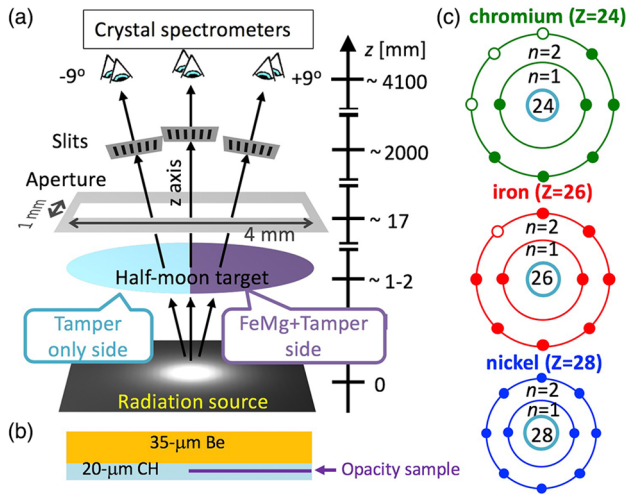


FIG. 1. (a) Opacity-experiment setup. (b) Target side view. (c) Dominant electron configurations of Cr, Fe, and Ni at achieved conditions. Vacancies in the shells are indicated by open circles.

Systematic opacity measurements across atomic number are a powerful way to address this problem. The experiment drives different elements to roughly the same T_e and n_e , but the atom's response to the conditions varies according to the nuclear binding energy. For example, in nickel (Ni: $Z = 28$), electrons are more tightly bound and more difficult to ionize and excite than for iron (Fe: $Z = 26$). Thus, the dominant charge state for Ni is the closed-shell Ne-like configuration [Fig. 1(c)]. In the closed-shell configurations, angular momentum coupling is appreciably simplified, theory is considered relatively accurate, and opacity is dominated by strong isolated lines. In contrast, as the atomic number is lowered to Fe or to chromium (Cr: $Z = 24$), the dominant charge states shift to open-shell F -like and N -like ions, respectively. These open-shell ions are computationally more challenging and increase opacity complexity. Furthermore, bound-electron wave functions of lower- Z elements extend farther from the nucleus and are more easily perturbed by plasma particles. Thus, measuring opacities of Cr, Fe, and Ni not only provides more data to test the experimental platform, but can also help identify possible opacity-model revisions. The value of systematic opacity studies has been recognized for two decades [25,26], but previous experiments were at lower T_e and n_e and did not satisfy benchmark-experiment criteria such as independent plasma diagnostics and reproducibility.

In this Letter we describe the first systematic benchmark opacity experiments as a function of atomic number, at stellar interior temperatures. Cr and Ni frequency-resolved opacities were measured. Analysis of comixed Mg spectra confirmed that T_e and n_e are nearly the same as those of Fe. Opacities are reproduced within 10%–20% from repeated experiments with varied sample thicknesses. Averaging opacity spectra over multiple experiments reduces the

uncertainty down to $\pm 6\%$ for Cr and $\pm 10\%$ for Ni. High reproducibility reflects smallness of experiment-to-experiment errors and demonstrates experiment-method reliability.

Furthermore, the data reveal intriguing atomic-number-dependent disagreements between data and models, which suggest three distinct opacity-model refinements. First, the opacity window disagreement is observed from Cr and Fe, but not from Ni. This suggests a calculational challenge for open L -shell configurations. Second, apparent line shape disagreements in all three elements suggest insufficient understanding of atomic interaction with plasma environment and/or the treatment of excited states. Third, the modeled quasicontinuum opacity at short wavelength agrees with Cr and Ni measurements, in contrast to the Fe result. The Fe data use the same experimental method and should be as reliable as Cr and Ni. Also, Fe models agreed with lower T_e/n_e measurements. Thus, these Cr, Fe, and Ni quasicontinuum results suggest either that models are missing opacity that becomes important at specific conditions that the high- T_e/n_e Fe experiments satisfied or there is an undetected systematic flaw unique to Fe experiments at high T_e/n_e .

The opacity experimental technique has evolved and improved over 30 years [25,27–37]. Typically, frequency-dependent opacity is inferred by measuring transmission through a heated sample. The sample transmission T_ν and opacity κ_ν are related to the source I_0 (backlight) and measured spectra I_ν :

$$T_\nu = I_\nu/I_0 = e^{-\kappa_\nu \rho L},$$

where ρL is the sample areal density.

The measurement requirements are extensive [11,18,32]. (1) The sample is uniformly heated to conditions of interest, achieving local-thermodynamic equilibrium. (2) Spectra (I_0 and I_ν) and sample areal density ρL need to be accurately measured. (3) The instrumental spectral resolving power has to be sufficiently high and accurately measured. (4) Backlight radiation and tamper transmission must be free of short-scale wavelength-dependent structure. (5) Impact of plasma self-emission must be minimized. (6) The tamper-transmission difference [18] must be minimized. (7) Sample temperature, density, and drive radiation must be independently diagnosed. (8) Measurements must be repeated with multiple sample thicknesses to ensure accurate opacity measurements over a wide dynamic range.

The Sandia National Laboratories' Z opacity platform [Fig. 1(a)] has been developed over the past decade to meet these criteria [11,12,14,15,38]. The semicircular half-moon sample (i.e., Fe, Cr, or Ni comixed with Mg) is sandwiched between circular low-opacity (CH and/or Be) tamping materials [tamper, Fig. 1(b)]. The sample areal density is measured using Rutherford backscattering

spectroscopy (RBS) within $\pm 4\%$ error. The sample is volumetrically heated by energetic photons from the Z radiation source [34] to achieve uniform, near-equilibrium conditions. At stagnation, the source provides spectrally smooth 350-eV Planckian-like backlight radiation, which overwhelms the 180-eV plasma emission. The sample-attenuated backlight radiation is measured by multiple, slit-imaged, crystal spectrometers fielded along 0° and $\pm 9^\circ$ [39] with respect to the sample normal. Each spectrometer records multiple spectrally and spatially resolved images with high signal-to-noise ratio (S/N). Thus, each experiment simultaneously records 16–36 spectral images that further improves S/N and reduces instrument artifacts. The setup provides sample-attenuated (I_ν at $+9^\circ$) and unattenuated (I_0 at -9°) spectra in each experiment.

Continuous investigations since BNLR15 support the experiment's reliability. The impact of temporal or spatial gradients, sample or tamper self-emission, and the potential difference in tamper transmission at the tamper-only side and opacity-sample-embedded side were numerically investigated and found to be negligible [18]. Uncertainties in the inferred T_e and n_e due to the choice of analysis model have minor impact on the reported model-data disagreements [16]. The validity of the assumed 1D expansion and the accuracy of RBS areal-density measurements were confirmed by good agreement between the Mg areal density inferred from Mg spectroscopy and that of the RBS measurement.

For further constraints, we performed and repeated six Cr and five Ni opacity experiments with varied sample thicknesses. The Cr data include four experiments with 3.2×10^{18} and two with 1.8×10^{18} Cr/cm². The Ni data include two experiments with 0.403×10^{18} and one each with 1.19×10^{18} , 2.30×10^{18} , and 3.74×10^{18} Ni/cm². Plasma conditions inferred from Mg spectroscopy [14] were $T_e = 181 \pm 6(3\%)$ eV and $n_e = (2.9 \pm 0.1) \times 10^{22}(3\%)$ cm⁻³ for Cr and $T_e = 187 \pm 6(3\%)$ eV and $n_e = (2.9 \pm 0.3) \times 10^{22}(10\%)$ cm⁻³ for Ni.

Checking reproducibility from different sample thicknesses is critical for (i) assessing the accuracy of the analysis method and (ii) confirming the reliability of the experimental method. Opacity is most accurately measured when transmission falls in the 0.15–0.85 range [18]. The opacity determination depends on the accuracy of the transmission determination, background subtraction, and sample areal density in nonlinear ways. Fortunately, these uncertainties affect the inferred opacity differently. Furthermore, their impact depends strongly on the transmission values and thus on the sample thickness. Thus, any significant systematic errors in those could be identified through the thickness dependence of the measured opacity.

The opacity is determined (see Ref. [11], [12], and Supplemental Material of Ref. [13]), including formal propagation of the three uncertainties. The transmission uncertainty is analytically determined from calibration-shot

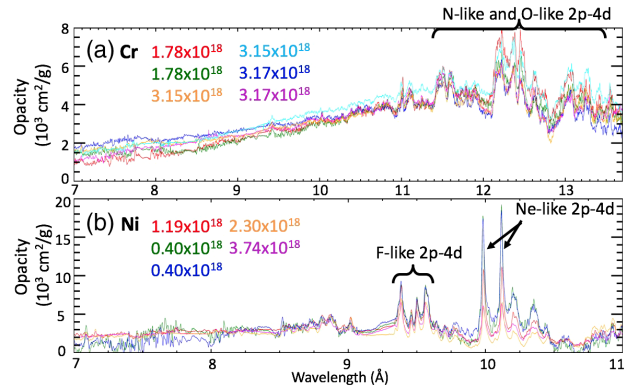


FIG. 2. Reproducibility in measured opacities for (a) Cr and (b) Ni. Each color corresponds to independent experiments with their sample areal densities (g/cm²) embedded in the figure.

statistics that are collected over a decade. Areal density is known within $\pm 4\%$ based on the RBS measurement and Mg spectroscopy. Line-saturation dependence on backlight brightness suggests that a $10 \pm 3\%$ background exists. The expected opacity values and its uncertainties are determined at every wavelength by propagating these uncertainties using Monte Carlo methods. Opacities inferred from repeated experiments agree within the inferred uncertainties, supporting the validity of the analysis and uncertainty values.

Furthermore, the small variation in experiment-to-experiment inferred opacity (Fig. 2) reflects the smallness of some systematic errors and all random errors. The excellent reproducibility supports the experiment reliability.

The OP opacity model [4,40] is widely available and extensively used for solar or stellar models [41]. Comparisons between OP and the measured opacities (Fig. 3) provide essential clues for model refinements. Over the measured spectral range, opacity is believed to be mostly contributed by bound-bound transitions ($\kappa_\nu^{\text{BB}} \propto \sum_l n_l f_{lu} \phi_{lu}(\nu)$) at long wavelengths and bound-free (BF) transitions ($\kappa_\nu^{\text{BF}} \propto \sum_l n_l \sigma_{lu}(\nu)$) at short wavelengths. n_l is a lower state population; f_{lu} and $\phi_{lu}(\nu)$ are the BB-transition oscillator strength and area-normalized spectral line shape from lower l to upper u states; σ_{lu} is the photoionization cross section from a state l to an ionized state u . Atomic data calculations affect f_{lu} , σ_{lu} , and BB line locations; population calculations affect n_l ; density can affect all of these parameters, but especially $\phi_{lu}(\nu)$.

The OP calculation disagrees with measured BB line locations for all three elements, revealing fundamental deficiency in the OP atomic structure. The atomic structure is the basis for accurate calculation of f_{lu} , σ_{lu} , n_l , and $\phi_{lu}(\nu)$, and its deficiency can impact the overall opacity-calculation accuracy.

While OP opacity (Fig. 3) is widely used by astrophysicists due to its accessibility, other opacity models can generate opacities with a more complete set of atomic

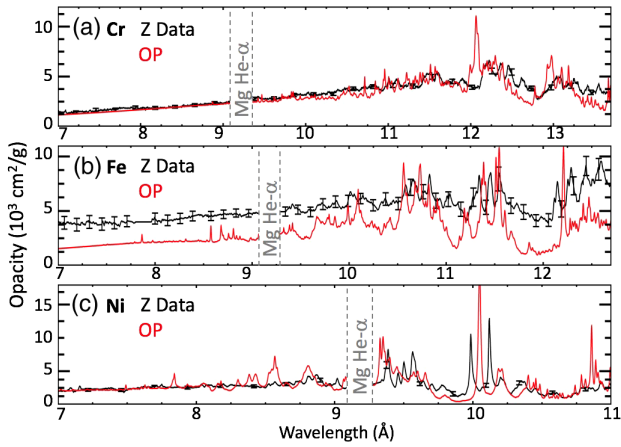


FIG. 3. Comparison of OP opacity (red line) and measured opacity (black line) approximately at 180 eV and $3 \times 10^{22} \text{ cm}^{-3}$ for (a) Cr, (b) Fe, and (c) Ni. Fe data and calculation are adopted from Fig. 3 of BNLR15. Opacities over 9.1–9.3 Å depend on the accuracy of Mg He- α removal and are not shown here. Wavelength upper limit is determined by the onset of strong lines from $n = 2 \rightarrow 3$ transitions, which are still under investigation.

levels [21,42]. Selected comparisons (Fig. 4) over the BB and window regions with ATOMIC [19], OPAS [43], SCO-RCG [44], SCRAM [45], and TOPAZ [46] show that all these models predict the BB transition energies more accurately than OP. A couple of these models are beginning to be used for detailed solar structure calculations [19, 47–52] though their codes are not publicly available. This large collection of models that employ diverse physics approaches can help to identify which physical approximations are most accurate.

The opacity window disagreement trend (Fig. 4, black arrows) suggests that models are challenged by open L -shell configurations, since the disagreement is not observed when ions are predominantly closed shell (i.e., Ni) [see Fig. 1(c)]. Inaccuracy in wavelengths, strengths, and widths for the multitude of weak BB transitions that arise in open L -shell configurations might lead to windows that are less filled in the model calculations than the data. This hypothesis can be tested by performing Ni experiments at higher temperature, moving the Ni plasma away from the closed-shell electronic configuration.

Calculated line shape accuracy $\phi_{lu}(\nu)$ is evaluated with the Ne-like Ni $2p$ - $4d$ line near 9.98 Å. This line is used because it is less blended with other lines and has relatively low continuum underneath. The area-normalized line shape for this transition measured in four experiments was reproducible to within 10% [Fig. 5(a)]. The two thick-sample measurements were not included in Fig. 5, since the lines are artificially broadened by the combination of the high line-center optical depth, line saturation, and finite instrument resolution. Figure 5(b) shows raw opacity calculations from four opacity models: ATOMIC, OPAS, SCO-RCG, and SCRAM. Some calculations are

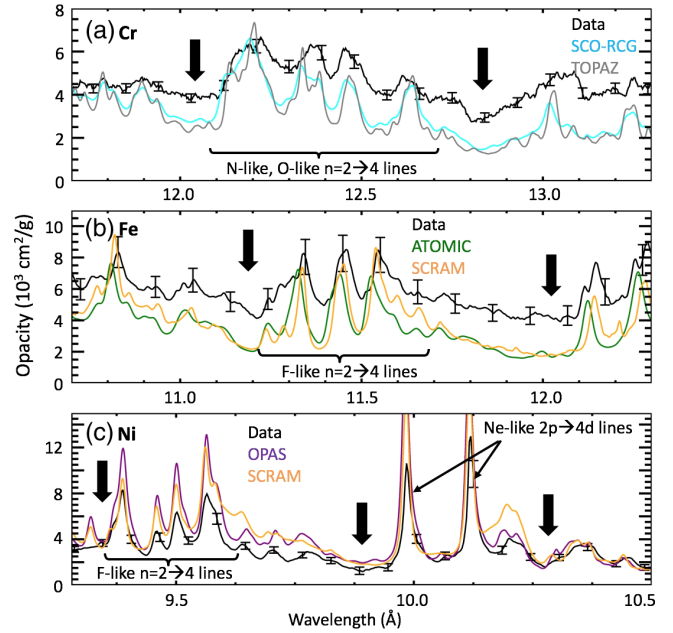


FIG. 4. Enlarged comparison of measured (black line) and modeled (colored lines) opacities for (a) Cr, (b) Fe, and (c) Ni over the window and $2p$ - $4d$ bound-bound lines. While only two models are compared in each plot for clarity, the level of disagreement is similar for all models. The opacity-window (black arrows) disagreement is not observed for Ni, potentially due to closed L -shell configuration.

already after major refinements, motivated by preliminary model-data comparison [53]. The FWHM predictions from these models vary by approximately a factor of 2. These calculated opacities are compared with the measurements by first converting to transmission, convolving with the measured instrumental resolution, and then converting back to opacity. Line shapes $\phi_{lu}(\nu)$ are extracted from the data and calculations by subtracting linear continuum and performing area normalization. While the line widths predicted by most models are significantly underestimated, SCO-RCG predictions agree well with the measured line shape [Fig. 5(c)]. A 60%–90% width increase for the other models is needed to bring them into agreement with the data and with SCO-RCG.

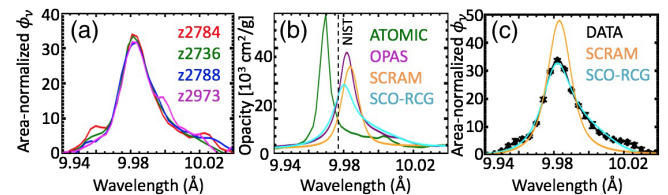


FIG. 5. (a) Reproducibility in Ne-like Ni $2p$ - $4d$ line shapes. (b) Model-dependent variation of calculated Ne-like Ni $2p$ - $4d$ line opacity (without instrument-broadening effects). (c) Comparisons of measured (black line) and modeled (colored lines) line shapes (with instrumental transmission resolution, see text). Only the broadest one shows good agreement; other models require 60%–90% extra broadening.

It is reasonable to expect similar width disagreements for other lines since models use the same method for them. Energy is transferred more readily in windows between narrow lines. Thus, if opacity models underestimate all line widths, this may partially explain why calculated opacities are lower than measured. In fact, almost all the lines do look broader in the data. However, further scrutiny is necessary to determine the accuracy of other line shapes.

The observed line shape disagreement indicates insufficient understanding of impact collisions by dynamic electrons, the static-ion Stark broadening, and/or satellite lines from excited states. Opacity models commonly compute electron broadening based on the Baranger [54] approximation. The ion Stark effect is neglected or crudely approximated [55], despite a recent publication [24] describing its potential importance. Satellite-line contributions are also computed differently from one model to another. Investigations are under way to identify which aspect of line-broadening theory is responsible for the reported line shape discrepancies.

The model-data comparison (Fig. 6) over the short-wavelength region shows that the systematically higher quasicontinuum opacity reported by BNLR15 is observed only from Fe. While this proves that the experiments are not always biased to measure higher-than-predicted continuum opacity, the question remains: Why is the predicted iron quasicontinuum lower than the data only for Fe and only at high T_e/n_e [12,13] ?

Currently, there are two hypotheses for this intriguing finding. One is that models miss some important physics that becomes significant at conditions satisfied by the high- T_e/n_e Fe experiments. The BF cross section has never been experimentally validated for highly ionized ions. Furthermore, the quasicontinuum has significant contribution from billions of weak BB lines from states where multiple bound electrons are in excited orbitals simultaneously [13]. Currently, there is no consensus on how many multiexcited states opacity models should include. The disagreement could also come from some neglected processes. For example, preliminary calculations of two-photon absorption [22] suggest that this neglected process would substantially increase the absorption. Another idea for missing physics was also recently published [56]. Refined

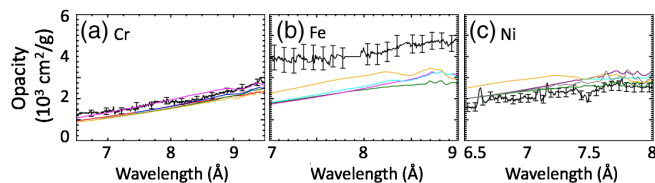


FIG. 6. Comparison of measured (black line) and modeled (colored lines) quasicontinuum opacities for (a) Cr, (b) Fe, and (c) Ni, revealing notable discrepancy only from Fe. Models: ATOMIC (green line), OPAS (purple line), SCO-RCG (cyan line), SCRAM (orange line), and TOPAZ (gray line).

calculations need to evaluate whether these suggested contributions are consistent with the entire Cr, Fe, and Ni dataset.

The other hypothesis is that there is an undetected error in the high- T_e/n_e Fe-opacity result. According to this hypothesis, the problem must not exist in the Cr, Ni, or lower-temperature Fe experiments since the modeled and measured quasicontinuum opacity agreed. This contradicts the assertion that the same methods were used for all the experiments. Nevertheless, it would be valuable to recheck the accuracy of BNLR15 by performing additional high- T_e/n_e Fe experiments, as well as revisiting the data analysis.

Ultimately, these complex results demonstrate the power of the systematic opacity study described here. Insisting that models and data should agree over a range of atomic numbers, temperatures, and densities is a powerful test for both opacity theory and experiment. This approach guides more accurate stellar interiors modeling and improved understanding of the internal structure of the Sun.

The implication of our measurements is significant for the Sun and many stars. Therefore, the measurements should be confirmed by independent experiments. However, this requires large HED facilities [57–59]. In addition, facility time and resources devoted must be sufficient to satisfy the key criteria reported here, such as high reproducibility and independent plasma diagnostics.

The authors are grateful to the Z experiment team, the management team, and the target fabrication teams at General Atomics and Los Alamos National Laboratories for their hard work and generous support. Sandia National Laboratories is a multimission laboratory managed and operated by National Technology and Engineering Solutions of Sandia, LLC., a wholly owned subsidiary of Honeywell International, Inc., for the U.S. Department of Energy’s National Nuclear Security Administration under Contract No. DE-NA-0003525. This Letter describes objective technical results and analysis. Any subjective views or opinions that might be expressed in the paper do not necessarily represent the views of the U.S. Department of Energy or the United States Government. Los Alamos National Laboratory is operated by Triad National Security, LLC, for the National Nuclear Security Administration of U.S. Department of Energy (Contract No. 89233218CNA000001).

*On leave from National Institute for Fusion Science, Toki, Gifu, Japan.

- [1] N. R. Simon, *Astrophys. J.* **260**, L87 (1982).
- [2] C. A. Iglesias, F. J. Rogers, and B. G. Wilson, *Astrophys. J.* **322**, L45 (1987).
- [3] C. A. Iglesias, F. J. Rogers, and B. G. Wilson, *Astrophys. J.* **360**, 221 (1990).

- [4] M. J. Seaton, Y. Yan, D. Mihalas, and A. K. Pradhan, *Mon. Not. R. Astron. Soc.* **266**, 805 (1994).
- [5] F. J. Rogers and C. A. Iglesias, *Science* **263**, 50 (1994).
- [6] F. J. Rogers and C. A. Iglesias, *Space Sci. Rev.* **85**, 61 (1998).
- [7] S. Salmon, J. Montalbán, T. Morel, A. Miglio, M.-A. Dupret, and A. Noels, *Mon. Not. R. Astron. Soc.* **422**, 3460 (2012).
- [8] E. Moravveji, *Mon. Not. R. Astron. Soc. Lett.* **455**, L67 (2016).
- [9] A. Hui-Bon-Hoa and S. Vauclair, *Astron. Astrophys.* **610**, L15 (2018).
- [10] S. Basu and H. M. Antia, *Phys. Rep.* **457**, 217 (2008).
- [11] J. E. Bailey, G. A. Rochau, R. C. Mancini, C. A. Iglesias, J. J. MacFarlane, I. E. Golovkin, C. Blancard, P. Cosse, and G. Faussurier, *Phys. Plasmas* **16**, 058101 (2009).
- [12] J. E. Bailey, G. A. Rochau, C. A. Iglesias, J. J. Abdallah, J. J. MacFarlane, I. Golovkin, P. Wang, R. C. Mancini, P. W. Lake, T. C. Moore, M. Bump, O. Garcia, and S. Mazevet, *Phys. Rev. Lett.* **99**, 265002 (2007).
- [13] J. E. Bailey *et al.*, *Nature (London)* **517**, 56 (2015).
- [14] T. Nagayama, J. E. Bailey, G. Loisel, S. B. Hansen, G. A. Rochau, R. C. Mancini, J. J. MacFarlane, and I. Golovkin, *Phys. Plasmas* **21**, 056502 (2014).
- [15] T. Nagayama, J. E. Bailey, G. Loisel, G. A. Rochau, and R. E. Falcon, *Rev. Sci. Instrum.* **85**, 11D603 (2014).
- [16] T. Nagayama *et al.*, *High Energy Density Phys.* **20**, 17 (2016).
- [17] T. Nagayama, J. E. Bailey, G. Loisel, G. A. Rochau, J. J. MacFarlane, and I. Golovkin, *Phys. Rev. E* **93**, 023202 (2016).
- [18] T. Nagayama, J. E. Bailey, G. P. Loisel, G. A. Rochau, J. J. MacFarlane, and I. E. Golovkin, *Phys. Rev. E* **95**, 063206 (2017).
- [19] J. Colgan, D. P. Kilcrease, N. H. Magee, M. E. Sherrill, J. J. Abdallah, P. Hakel, C. J. Fontes, J. A. Guzik, and K. A. Mussack, *Astrophys. J.* **817**, 116 (2016).
- [20] S. N. Nahar and A. K. Pradhan, *Phys. Rev. Lett.* **116**, 235003 (2016).
- [21] C. A. Iglesias and S. B. Hansen, *Astrophys. J.* **835**, 284 (2017).
- [22] R. M. More, S. B. Hansen, and T. Nagayama, *High Energy Density Phys.* **24**, 44 (2017).
- [23] D. P. Kilcrease, J. Colgan, P. Hakel, C. J. Fontes, and M. E. Sherrill, *High Energy Density Phys.* **16**, 36 (2015).
- [24] R. C. Mancini, *J. Phys. Conf. Ser.* **717**, 012069 (2016).
- [25] G. Winhart, K. Eidmann, C. A. Iglesias, and A. Bar-Shalom, *Phys. Rev. E* **53**, R1332 (1996).
- [26] G. Loisel, P. Arnault, S. Bastiani Ceccotti, T. Blenski, T. Caillaud, J. Fariaut, W. Fölsner, F. Gilleron, J. C. Pain, M. Poirier, C. Reverdin, V. Silvert, F. Thais, S. Turck-Chieze, and B. Villette, *High Energy Density Phys.* **5**, 173 (2009).
- [27] S. J. Davidson, J. M. Foster, C. C. Smith, K. A. Warburton, and S. J. Rose, *Appl. Phys. Lett.* **52**, 847 (1988).
- [28] T. S. Perry, S. J. Davidson, F. J. D. Serduke, D. R. Bach, C. C. Smith, J. M. Foster, R. J. Doyas, R. A. Ward, C. A. Iglesias, F. J. Rogers, J. Abdallah, R. E. Stewart, J. D. Kilkenny, and R. W. Lee, *Phys. Rev. Lett.* **67**, 3784 (1991).
- [29] J. M. Foster, D. J. Hoarty, C. C. Smith, P. A. Rosen, S. J. Davidson, S. J. Rose, T. S. Perry, and F. J. D. Serduke, *Phys. Rev. Lett.* **67**, 3255 (1991).
- [30] L. B. Da Silva, B. J. MacGowan, D. R. Kania, B. A. Hammel, C. A. Back, E. Hsieh, R. Doyas, C. A. Iglesias, F. J. Rogers, and R. W. Lee, *Phys. Rev. Lett.* **69**, 438 (1992).
- [31] P. Springer, D. Fields, B. Wilson, J. Nash, W. Goldstein, C. A. Iglesias, F. J. Rogers, J. Swenson, M. Chen, A. Bar-Shalom, and R. Stewart, *Phys. Rev. Lett.* **69**, 3735 (1992).
- [32] T. Perry *et al.*, *Phys. Rev. E* **54**, 5617 (1996).
- [33] P. T. Springer, K. L. Wong, C. A. Iglesias, J. H. Hammer, J. L. Porter, A. Toor, W. H. Goldstein, B. G. Wilson, F. J. Rogers, C. Deeney, D. S. Dearborn, C. Bruns, J. Emig, and R. E. Stewart, *J. Quant. Spectrosc. Radiat. Transfer* **58**, 927 (1997).
- [34] C. Chenais Popovics, H. Merdji, T. Missalla, F. Gilleron, J. C. Gauthier, T. Blenski, F. Perrot, M. Klapisch, C. Bauche-Arnoult, J. Bauche, A. Bachelier, and K. Eidmann, *Astrophys. J. Suppl. Ser.* **127**, 275 (2000).
- [35] C. Chenais-Popovics, M. Fajardo, F. Gilleron, U. Teubner, J. C. Gauthier, C. Bauche-Arnoult, A. Bachelier, J. Bauche, T. Blenski, F. Thais, F. Perrot, A. Benuzzi, S. Turck-Chieze, J. P. Chièze, F. Dorchies, U. Andiel, W. Foelsner, and K. Eidmann, *Phys. Rev. E* **65**, 016413 (2001).
- [36] J. E. Bailey, P. Arnault, T. Blenski, G. Dejonghe, O. Peyrusse, J. J. MacFarlane, R. C. Mancini, M. E. Cuneo, D. S. Nielsen, and G. A. Rochau, *J. Quant. Spectrosc. Radiat. Transfer* **81**, 31 (2003).
- [37] P. Renaudin, C. Blancard, J. Bruneau, G. Faussurier, J. E. Fuchs, and S. Gary, *J. Quant. Spectrosc. Radiat. Transfer* **99**, 511 (2006).
- [38] J. E. Bailey, G. A. Rochau, R. C. Mancini, C. A. Iglesias, J. J. MacFarlane, I. E. Golovkin, J. C. Pain, F. Gilleron, C. Blancard, P. Cosse, G. Faussurier, G. A. Chandler, T. J. Nash, D. S. Nielsen, and P. W. Lake, *Rev. Sci. Instrum.* **79**, 113104 (2008).
- [39] G. Loisel, J. E. Bailey, G. A. Rochau, G. S. Dunham, L. B. Nielsen-Weber, and C. R. Ball, *Rev. Sci. Instrum.* **83**, 10E133 (2012).
- [40] N. R. Badnell, M. A. Bautista, K. Butler, F. Delahaye, C. Mendoza, P. Palmeri, C. J. Zeippen, and M. J. Seaton, *Mon. Not. R. Astron. Soc.* **360**, 458 (2005).
- [41] A. M. Serenelli, *Astrophys. Space Sci.* **328**, 13 (2010).
- [42] C. Blancard, J. Colgan, P. Cosse, G. Faussurier, C. J. Fontes, F. Gilleron, I. Golovkin, S. B. Hansen, C. A. Iglesias, D. P. Kilcrease, J. J. MacFarlane, R. M. More, J. C. Pain, M. Sherrill, and B. G. Wilson, *Phys. Rev. Lett.* **117**, 249501 (2016).
- [43] C. Blancard, P. Cossé, and G. Faussurier, *Astrophys. J.* **745**, 10 (2012).
- [44] J.-C. Pain and F. Gilleron, *High Energy Density Phys.* **15**, 30 (2015).
- [45] S. Hansen, J. Bauche, C. Bauche-Arnoult, and M. F. Gu, *High Energy Density Phys.* **3**, 109 (2007).
- [46] C. A. Iglesias, *High Energy Density Phys.* **15**, 4 (2015).
- [47] G. Mondet, C. Blancard, P. Cossé, and G. Faussurier, *Astrophys. J. Suppl. Ser.* **220**, 2 (2015).

- [48] M. Le Pennec, S. Turck-Chieze, S. Salmon, C. Blancard, P. Cossé, G. Faussurier, and G. Mondet, *Astrophys. J.* **813**, L42 (2015).
- [49] P. Walczak, C. J. Fontes, J. Colgan, D. P. Kilcrease, and J. A. Guzik, *Astron. Astrophys.* **580**, L9 (2015).
- [50] J. Daszyńska-Daszkiewicz, A. A. Pamyatnykh, P. Walczak, J. Colgan, C. J. Fontes, and D. P. Kilcrease, *Mon. Not. R. Astron. Soc.* **466**, 2284 (2017).
- [51] G. Buldgen, S. J. A. J. Salmon, M. Godart, A. Noels, R. Scouflaire, M.-A. Dupret, D. R. Reese, J. Colgan, C. J. Fontes, P. Eggenberger, P. Hakel, D. P. Kilcrease, and O. Richard, *Mon. Not. R. Astron. Soc. Lett.* **472**, L70 (2017).
- [52] G. Buldgen, S. J. A. J. Salmon, A. Noels, R. Scouflaire, D. R. Reese, M.-A. Dupret, J. Colgan, C. J. Fontes, P. Eggenberger, P. Hakel, D. P. Kilcrease, and S. Turck-Chieze, *Astron. Astrophys.* **607**, A58 (2017).
- [53] T. Nagayama, J. E. Bailey, C. Blancard, J. Colgan, Ph. Cossé, G. Faussurier, C. J. Fontes, F. Gilleron, S. B. Hansen, C. A. Iglesias, D. P. Kilcrease, J.-C. Pain, M. E. Sherrill, and B. G. Wilson (private communication).
- [54] M. Baranger, *Phys. Rev.* **112**, 855 (1958).
- [55] B. F. Rozsnyai, *J. Quant. Spectrosc. Radiat. Transfer* **17**, 77 (1977).
- [56] P. Liu, C. Gao, Y. Hou, J. Zeng, and J. Yuan, *Communications Physics* **1**, 95 (2018).
- [57] E. M. Campbell and W. J. Hogan, *Plasma Phys. Controlled Fusion* **41**, B39 (1999).
- [58] J.-L. Miquel, C. Lion, and P. Vivini, *J. Phys. Conf. Ser.* **688**, 012067 (2016).
- [59] N. W. Hopps, T. H. Bett, N. Cann, C. N. Danson, S. J. Duffield, D. A. Egan, S. P. Elsmere, M. T. Girling, E. J. Harvey, D. I. Hillier, D. J. Hoarty, P. M. R. Jinks, M. J. Norman, S. J. F. Parker, P. A. Treadwell, and D. N. Winter, in *High Power Lasers for Fusion Research*, edited by A. A. S. Awwal, A. M. Dunne, H. Azechi, and B. E. Kruschwitz (International Society for Optics and Photonics, 2011), p. 79160C.